The SUMO-specific isopeptidase SENP2 associates dynamically with nuclear pore complexes through interactions with karyopherins and the Nup107-160 nucleoporin subcomplex

Jacqueline Goeres[a], Pak-Kei Chan[b], Debaditya Mukhopadhyay[a], Hong Zhang[a], Brian Raught[b], and Michael J. Matunis[a]

[a]Department of Biochemistry and Molecular Biology, Bloomberg School of Public Health, Johns Hopkins University, Baltimore, MD 21205; [b]Ontario Cancer Institute, University of Toronto, Toronto, ON M5G 1L7, Canada

ABSTRACT The association of small, ubiquitin-related modifier–specific isopeptidases (also known as sentrin-specific proteases, or SENPs) with nuclear pore complexes (NPCs) is conserved in eukaryotic organisms ranging from yeast to mammals. However, the functional significance of this association remains poorly understood, particularly in mammalian cells. In this study, we have characterized the molecular basis for interactions between SENP2 and NPCs in human cells. Using fluorescence recovery after photobleaching, we demonstrate that SENP2, although concentrated at the nuclear basket, is dynamically associated with NPCs. This association is mediated by multiple targeting elements within the N-terminus of SENP2 that function cooperatively to mediate NPC localization. One of these elements consists of a high-affinity nuclear localization signal that mediates indirect tethering to FG-repeat–containing nucleoporins through karyopherins. A second element mediates interactions with the Nup107-160 nucleoporin subcomplex. A third element consists of a nuclear export signal. Collectively, our findings reveal that SENP2 is tethered to NPCs through a complex interplay of interactions with nuclear import and export receptors and nucleoporins. Disruption of these interactions enhances SENP2 substrate accessibility, suggesting an important regulatory node in the SUMO pathway.

INTRODUCTION

Small, ubiquitin-related modifiers (SUMOs) are ~100–amino acid proteins that covalently and reversibly attach to lysine residues in substrate proteins to modulate their localization, activity, and/or stability (Johnson, 2004; Geiss-Friedlander and Melchior, 2007). Genetic and proteomic studies have identified hundreds of SUMO substrates, implicating sumoylation as an essential regulator of a wide array of cellular processes, including transcription, chromatin structure, DNA repair, chromosome segregation, stress response, and nucleocytoplasmic transport (Golebiowski *et al.*, 2009; Makhnevych *et al.*, 2009). Sumoylation is achieved through a three-step enzymatic cascade involving an ATP-dependent E1-activating enzyme (the Aos1/Uba2 heterodimer), an E2-conjugating enzyme (Ubc9), and in many cases, one of several E3 ligases (Johnson, 2004). Reversal of this modification is achieved by a family of SUMO-specific

isopeptidases (referred to as sentrin-specific proteases, or SENPs, in vertebrates; Mukhopadhyay and Dasso, 2007).

While there are two SUMO-specific isopeptidases in yeasts, Ulp1 and Ulp2, mammalian genomes encode six: SENP1, SENP2, SENP3, SENP5, SENP6, and SENP7. Each of these enzymes contains a highly conserved C-terminal catalytic domain but is distinguished by a distinct N-terminal domain that targets it to a unique subcellular location (Mukhopadhyay and Dasso, 2007). Ulp1, SENP1, and SENP2 are localized to nuclear pore complexes (NPCs), while Ulp2, SENP6, and SENP7 localize throughout the nucleoplasm (Li and Hochstrasser, 1999, 2000, 2003; Hang and Dasso, 2002; Zhang et al., 2002; Bailey and O'Hare, 2004; Mukhopadhyay and Dasso, 2007; Kroetz et al., 2009). Vertebrates contain a unique pair of nucleolar-specific isopeptidases, SENP3 and SENP5 (Nishida et al., 2000; Gong and Yeh, 2006). Studies in yeast have demonstrated clearly that the regulated localization of SUMO-specific isopeptidases serves to define their functions by restricting access to protein substrates (Li and Hochstrasser, 2000, 2003; Makhnevych et al., 2007; Kroetz et al., 2009). How subcellular localization affects the functions of each of the six mammalian SUMO-specific isopeptidases, however, remains to be fully characterized.

The conserved localization of SUMO-specific isopeptidases at NPCs implies a functional link between sumoylation and nucleocytoplasmic transport (Hang and Dasso, 2002; Zhang et al., 2002; Li and Hochstrasser, 2003; Panse et al., 2003; Smith et al., 2004; Xu et al., 2007). Consistent with this link, the SUMO E2-conjugating enzyme Ubc9 and the E3 ligase RanBP2/Nup358 also localize to NPCs (Pichler et al., 2002; Zhang et al., 2002). NPCs are massive protein complexes that permeate the nuclear envelope and provide a selective passageway for the transport of proteins and RNAs into and out of the nucleus (Brohawn et al., 2009; Strambio-De-Castillia et al., 2010). Signal-mediated transport through NPCs is dependent on a family of soluble transport receptors called karyopherins (or importins and exportins) that bind to nuclear localization or export sequences (NLSs or NESs) in cargo proteins and facilitate their translocation through NPCs via interactions with FG repeat–containing nucleoporins (Terry et al., 2007). In the budding yeast, mutants deficient for sumoylation exhibit defects in the nuclear import of proteins containing classical NLSs due to impaired recycling of Kap60 (karyopherin-α; Stade et al., 2002). Exactly how sumoylation affects karyopherin recycling and/or NPC function remains to be fully understood.

In addition to affecting nucleocytoplasmic transport in yeast, sumoylation at NPCs has also been determined to be important for proper regulation of mRNA export and DNA repair. In particular, mutations affecting the localization of Ulp1 at NPCs also affect the retention of unspliced mRNAs in the nucleus and NPC-coupled DNA repair processes (Zhao and Blobel, 2005; Lewis et al., 2007; Palancade et al., 2007; Nagai et al., 2008). The localization of Ulp1 with NPCs has been studied extensively and shown to involve a complex network of interactions. Two domains in the N-terminus of Ulp1 mediate unconventional interactions with the nuclear transport receptors Kap60/Kap95 (karyopherin-α/β) and Kap121 (Pse1; Li and Hochstrasser, 2003; Panse et al., 2003). These receptors target Ulp1 to NPCs, where its association is dependent upon a subset of nucleoporins and NPC-associated proteins that include Nup60, the Nup84 nucleoporin subcomplex, Mlp1/Mlp2, and Esc1 (Zhao et al., 2004; Lewis et al., 2007; Palancade et al., 2007). Although the proper localization of Ulp1 to NPCs is critical for mRNA surveillance and DNA repair, the roles that sumoylation and desumoylation play in these processes remain poorly understood. Also, whether the localization of SUMO-specific isopeptidases in mammalian cells is similarly important for these processes remains to be determined.

While Ulp1 is localized to NPCs during interphase, it is released and relocalizes to the septin ring during mitosis, a targeting event dependent on interactions with Kap121 (Makhnevych et al., 2007). In addition, Ulp1 is released from NPCs in response to ethanol stress and relocalizes to nucleoli, a process mediated in part by interactions with Kap60/Kap95 (Sydorskyy et al., 2010). The localization of Ulp1 and its access to distinct subsets of sumoylated proteins are therefore subject to regulation and affected by its association with nuclear transport receptors.

Unlike Ulp1, relatively little is known about the association and functions of its vertebrate counterparts, SENP1 and SENP2, at NPCs. Previous work demonstrated that SENP2 is essential for embryonic development in mice, underscoring the importance of understanding its cellular functions (Kang et al., 2010). In cultured cells, SENP2 has been shown to shuttle between the nucleus and the cytoplasm and to concentrate at the nucleoplasmic face of NPCs through interactions with Nup153 (Hang and Dasso, 2002; Zhang et al., 2002; Itahana et al., 2006). Whether interaction with Nup153 is the sole determinant of SENP2 localization at NPCs, and whether this interaction is direct or indirect, was unknown. In this study, we provide a more detailed analysis of the molecular interactions between SENP2 and NPCs. Our findings reveal that SENP2 contains a high-affinity NLS that mediates unconventional interactions with nuclear transport receptors and tethering to FG-repeat nucleoporins. We also demonstrate that SENP2 contains a second NPC-targeting signal that mediates interactions with the Nup107-160 nucleoporin subcomplex, a subcomplex with essential functions in interphase NPC assembly and mitotic chromosome segregation. Our findings indicate that a complex network of interactions define the steady-state association of SENP2 with NPCs and suggest possible new functions for SENP2, as well as mechanisms for regulating its substrate selectivity.

RESULTS

Endogenous SENP2 localizes to NPCs, the nucleoplasm, and the cytoplasm

Exogenously expressed vertebrate SENP2 has been described as localizing to the nucleoplasm, cytoplasm, and NPC (Nishida et al., 2001; Hang and Dasso, 2002; Zhang et al., 2002; Itahana et al., 2006). To characterize the localization of endogenous SENP2, we produced rabbit polyclonal antibodies and demonstrated specificity by immunoblot analysis of untransfected and green fluorescent protein (GFP)-SENP2 transfected cell lysates. The antibody recognized GFP-SENP2, as well as multiple lower-molecular-weight bands in lysates of transfected and untransfected HeLa cells (Figure 1A). Four of the lower-molecular-weight bands were reduced upon transfection of three different RNA interference (RNAi) oligos directed against SENP2 in HEK293 and HeLa cells: one major band at 50 kDa and three additional bands at 60, 45, and 44 kDa (Figure 1B; unpublished data). We confirmed that these bands corresponded to different molecular-weight forms of SENP2 by treating lysates with a SUMO-2 vinyl sulfone derivative (SUMO-2-VS; Figure 1B). SUMO-2-VS forms a covalent intermediate with SUMO isopeptidases, resulting in a ~20-kDa shift in molecular weight (Mukhopadhyay et al., 2006). All four specific bands shifted upon treatment with SUMO2-VS, indicating that each protein contains isopeptidase activity. The different forms of SENP2 may arise through alternative splicing, as documented in mouse cells (Nishida et al., 2001; Best et al., 2002).

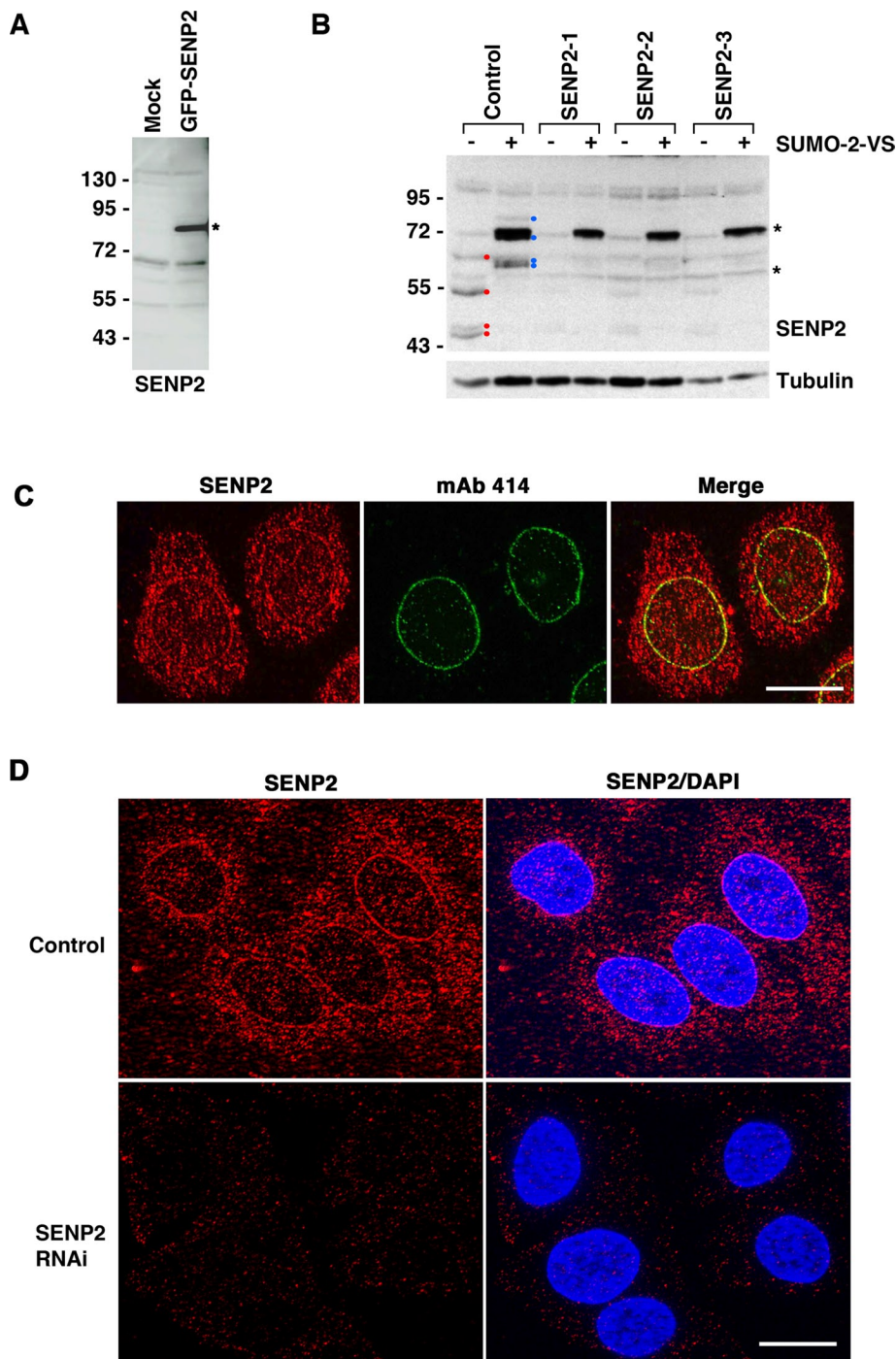We next examined the localization of endogenous SENP2 by indirect immunofluorescence microscopy. Endogenous SENP2 was

FIGURE 1: Characterization of endogenous SENP2. (A) Lysates of untransfected or GFP-SENP2–transfected HeLa cells were resolved by SDS–PAGE and immunoblot analysis was performed using SENP2-specific polyclonal antibodies. *, GFP-SENP2. (B) HEK293 cells were transfected with scramble (Control) or one of three SENP2-specific siRNA oligos. Cell extracts were incubated in the absence (−) or presence (+) of HA-tagged SUMO-2-VS for 30 min. Reactions were terminated by addition of SDS sample buffer and resolved by SDS–PAGE. Immunoblot analysis was performed using SENP2-specific antibodies. Red dots, RNAi-sensitive bands; blue dots, SUMO-2-VS shifted bands; *, nonspecific bands. (C) HeLa cells were stained with antibodies specific for SENP2 and nucleoporins (mAb 414) and analyzed by indirect immunofluorescence microscopy. Scale bar: 10 μm. (D) HeLa cells were transfected with scramble (Control) or SENP2-specific siRNA oligos and examined by indirect immunofluorescence microscopy using SENP2-specific polyclonal antibodies. Images were taken using identical exposure settings. Scale bar: 10 μm.

concentrated at the nuclear envelope in interphase cells, where it colocalized with FG-repeat nucleoporins recognized by mAb 414 (Davis and Blobel, 1986; Figure 1C). In addition, diffuse staining was detected throughout the cytoplasm and nucleoplasm. NPC staining, as well as much of the diffuse nucleoplasmic and cytoplasmic signals, was markedly decreased in cells transfected with SENP2 small interfering RNAs (siRNAs; Figure 1D). Consistent with previous findings (Hang and Dasso, 2002; Zhang et al., 2002), transiently expressed, full-length GFP-SENP2 localized predominantly to NPCs (see Figure 3A later in the paper). Our findings reveal that human cells express multiple isoforms of SENP2 and suggest that specific isoforms may differentially distribute among NPCs, the nucleus, and the cytoplasm.

SENP2 contains multiple NPC-targeting signals

The N-terminal domain of SENP2 is necessary and sufficient for NPC localization (Hang and Dasso, 2002; Zhang et al., 2002). To further define and characterize NPC-targeting elements, we generated a series of N- and C-terminal SENP2 truncation expression constructs (Figure 2). Localization of GFP-SENP2 truncation mutants at NPCs was examined by colocalization with mAb 414 in HeLa cells. As previously reported, fusion of the N-terminal 63 amino acids of SENP2 to GFP was sufficient for NPC localization (Figure 3E; Hang and Dasso, 2002; Zhang et al., 2002). A notable increase in nucleoplasmic signal was also detected relative to full-length SENP2, suggesting that residues in addition to 1–63 may contribute to NPC interactions. Consistent with this, deletion of the N-terminal 63 amino acids from SENP2 (NΔ63) resulted in a notable increase in cytoplasmic and nucleoplasmic staining without completely abolishing NPC localization (Figure 3B). Deletion of the N-terminal 143 amino acids from SENP2 (NΔ143) had a similar effect (Figure 3C). Expression of the catalytic domain of SENP2 alone fused to GFP (NΔ367), however, resulted in predominantly diffuse nucleoplasmic localization with no apparent NPC targeting (Figure 3D).

These results indicate that residues 1–63, as well as a second signal located between residues 143–367, specify NPC targeting. Supporting the presence of a second signal, fusion of residues 143–350 to GFP resulted in NPC localization, as well as diffuse nucleoplasmic, nucleolar, and cytoplasmic localization (Figure 3F). A SENP2 mutant containing the first 63 amino acids but lacking
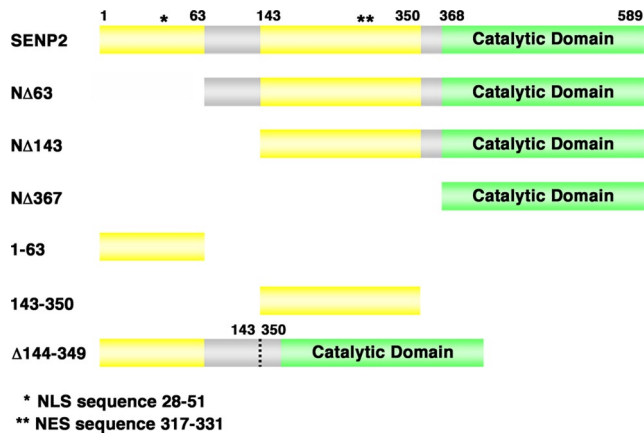
FIGURE 2: Schematic representations of SENP2 truncation mutants. The indicated SENP2 truncation mutants were generated using PCR and subcloned into the pEGFP-C1 vector. Features and domains of SENP2, including the catalytic domain (green), NLS, and NES motifs and defined NPC-targeting regions (yellow) are indicated.

residues 144–349 (Δ144–349) localized to NPCs, indicating that both NPC-targeting signals are self-sufficient (Figure 3G).

SENP2 interacts with karyopherins and nucleoporins

To identify SENP2-interacting proteins involved in SENP2's association with NPCs we used an affinity purification–mass spectrometry (AP-MS) approach (Gingras *et al.*, 2007). Tetracycline-inducible stable cell lines expressing full-length, Flag-tagged SENP2 were established. Following induction in two independently isolated lines, Flag-tagged SENP2 was immunopurified under nondenaturing purification conditions. SENP2-interacting proteins were analyzed by liquid chromatography, which was followed by tandem mass spectrometry (LC-MS/MS). Cells expressing the Flag tag alone or unrelated proteins were analyzed simultaneously, and only those proteins found specifically in Flag-tagged SENP2-expressing cells are reported (Table 1). Spectral counts, corresponding to the number of times a peptide from each protein was observed, are indicated, providing a rough approximation of relative abundance. Multiple nuclear transport receptors, including karyopherin-β_1, -β_2; karyopherin-α_1, -α_2, α_3, -α_4, and -α_6; and the karyopherin-α recycling factor CSE1L, were identified. In addition, a subset of FG repeat–containing nucleoporins (Nup153, Nup50, and Nup358/RanBP2) and members of the Nup107-160 subcomplex copurified specifically with Flag-SENP2. A variety of other putative interacting proteins were also identified, including proteins involved in splicing, transcription, and the cytoskeletal functions.

To define interacting partners specific to each of the two identified NPC-localization signals, we generated stable cell lines expressing SENP2 truncation mutants, including the N-terminus alone (amino acids [aa], 1–350), the catalytic domain alone (aa 350–589), and an internal deletion mutant lacking residues acids 144–349. As with full-length SENP2, proteins interacting with these mutants were identified by AP-MS. Proteins interacting with the N-terminal domain of SENP2 were similar to those observed with the full-length protein. Consistent with NPC-targeting signals being located within the N-terminal domain, associations with karyopherins and nucleoporins were retained (Table 1). Analysis of the catalytic domain alone revealed interactions with the subset of assorted "other" proteins found to interact with full-length SENP2. The internal deletion mutant, SENP2 Δ144-349, retained its interactions with karyopherins

and FG repeat–containing nucleoporins but not with members of the Nup107-160 subcomplex.

Previous studies identified a functional NLS in the N-terminus of SENP2 between amino acids 28 and 52 (Itahana *et al.*, 2006). To address whether this NLS mediates SENP2-karyopherin and nucleoporin interactions, we mutated two critical residues in this signal (R29A/R49A) and identified binding partners of the resulting protein using AP-MS. This mutant did not copurify with karyopherins, indicating that the NLS is required either directly or indirectly for karyopherin binding (Table 1). The NLS mutant also failed to copurify with FG repeat–containing nucleoporins, indicating that SENP2 interactions with these nucleoporins are likely to be karyopherin-mediated. Peptides derived from two members of the Nup107-160 subcomplex were, however, still detected.

The N-terminal NLS of SENP2 is a high-affinity, karyopherin-α–binding NLS

The N-terminal NLS in SENP2 is a bipartite signal with an unusually long and negatively charged spacer segment. At a basic level, this sequence bears resemblance to a subclass of NLSs found in proteins called karyopherin-α–releasing factors (KaRFs; Figure 4A). These proteins, which include Nup2 in yeast and Nup50 in vertebrates, are characterized by a high-affinity bipartite NLS capable of displacing cargo containing a classical NLS (Gilchrist *et al.*, 2002; Matsuura *et al.*, 2003; Matsuura and Stewart, 2005).

To investigate the nature of the interactions between the N-terminal NLS of SENP2 and karyopherin-α, recombinant glutathione S-transferase (GST)-tagged SENP2 1-63 or the NLS mutant, SENP2 1-63(R29A/R49A), were immobilized on glutathione beads and incubated with increasing concentrations of purified His-tagged karyopherin-α_2. The N-terminal 63 amino acids of SENP2 interacted robustly with karyopherin-α alone in an NLS-dependent manner (Figure 4B). To investigate whether SENP2 could function as a KaRF, binding competition assays were performed. Biotinylated karyopherin-α was preincubated with an excess of maltose-binding protein (MBP)-tagged SV40 NLS and subsequently with increasing concentrations of GST-tagged SENP2 1-63 (ranging from a 0.5:1 to a 4:1 M ratio of SENP2:NLS). Karyopherin-α/NLS complexes were captured using streptavidin-agarose beads and analyzed by immunoblot analysis. A reciprocal experiment was also performed in which karyopherin-α was preincubated with excess SENP2 1-63 and increasing concentrations of the SV40 NLS were titrated into the reaction. Consistent with having a high-affinity NLS with KaRF-like activity, SENP2 1-63 displaced the SV40 NLS from karyopherin-α. Excess SV40 NLS, however, did not displace SENP2 1-63 in the reciprocal experiment (Figure 4C). We also investigated the Ran-GTP sensitivity of a karyopherin-α/β heterodimer complexed with SENP2. Unlike the Ran-GTP–insensitive association of yeast Ulp1 with both Kap95 (karyopherin-β) and Kap60 (karyopherin-α; Panse *et al.*, 2003), Ran-GTP displaced karyopherin-β from SENP2. Karyopherin-α binding, however, was unaffected (Figure 4D).

To address whether individual karyopherins and nucleoporins associate directly with SENP2 or indirectly through extended protein complexes, we repeated the AP-MS analysis of wild-type SENP2, this time performing the purifications in both the presence and absence of nonhydrolyzable Ran-GTP. We anticipated that Ran-GTP would displace karyopherins associated indirectly with SENP2, but not karyopherins bound with high affinity to the N-terminal NLS, as shown above. Using spectral counts as an indicator of relative abundance, we detected significant reductions in the copurification of karyopherin-β_1 and -α_2 in the presence of Ran-GTP, as well as the
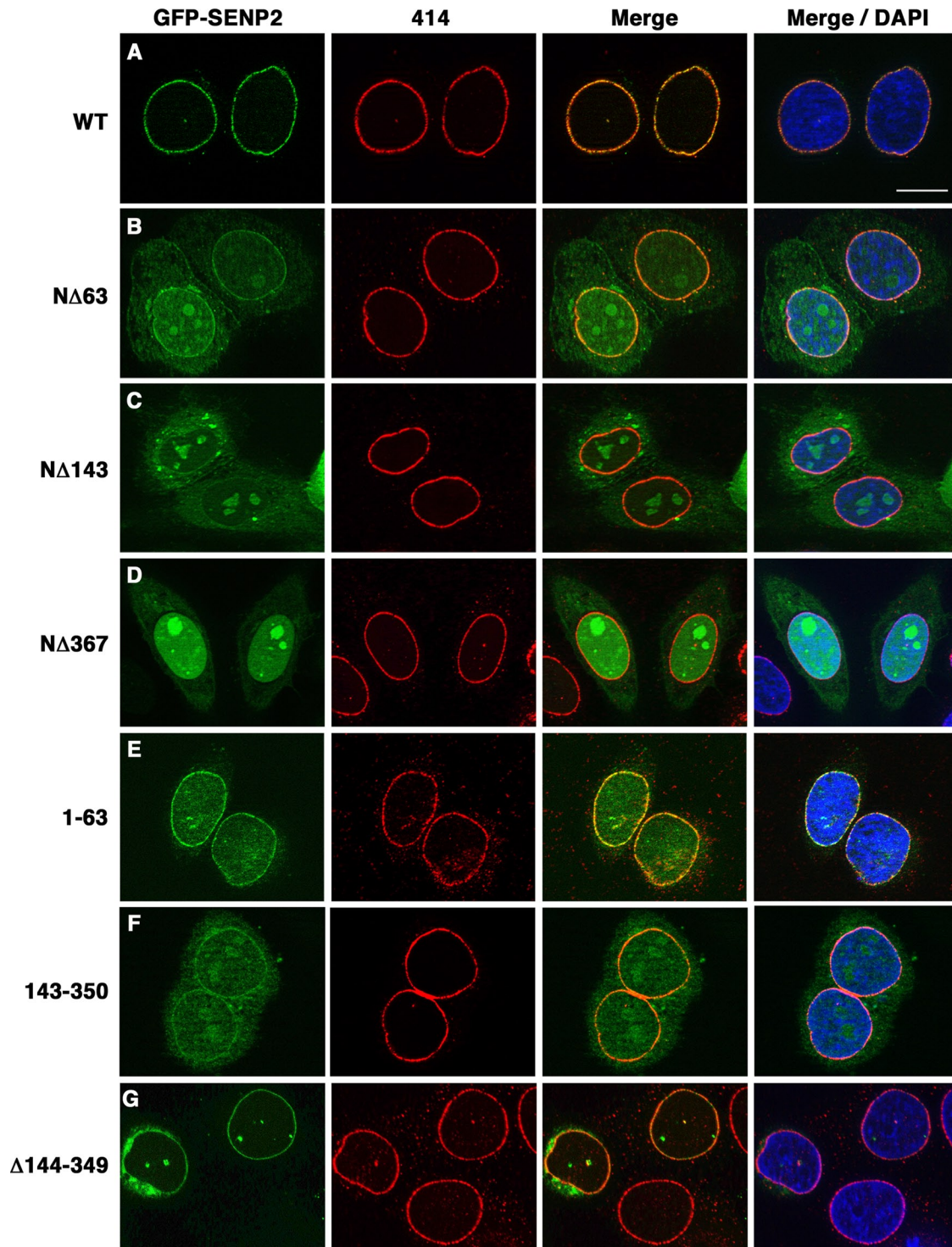
FIGURE 3: SENP2 contains multiple N-terminal NPC-targeting signals. HeLa cells were transfected with constructs coding for wild-type GFP-SENP2 or the indicated GFP-SENP2 deletion mutants. Colocalization with FG repeat–containing nucleoporins was determined by labeling cells with mAb 414 and by indirect immunofluorescence microscopy analysis. DNA was detected by staining with DAPI. Scale bar: 10 μm.

FG-repeat nucleoporins, Nup358 and Nup153 (Figure 4E). We detected no significant reductions in the levels of karyopherin-α_3 and -α_4, suggesting SENP2 associates directly with a distinct subfamily of karyopherins. Levels of Nup133 remained unaffected, consistent with SENP2 forming a direct association with the Nup107 complex.

Nuclear transport receptors mediate interactions between SENP2 and nucleoporins

To further verify and characterize SENP2-interacting proteins, immunopurification and immunoblotting experiments were performed. GFP-tagged, full-length SENP2 and SENP2 1-63, as well as the NLS mutants SENP2(R29A/R49A) and SENP2 1-63(R29A/R49A),

TABLE 1: Flag-tagged SENP2 wild-type and indicated mutants, spectral counts across immunopurification conditions.

Interacting partner groups	Gene ID	Protein ID	Gene name	FL poolA pelletA run1	FL poolA pelletA run2	FL poolB pelletB run1	FL poolB pelletB run2	FL poolB pelletC run1	FL poolB pelletC run2	FL poolC pelletB run1	FL poolC pelletB run2	1-350 poolB pelletA run1	1-350 poolB pelletA run2	1-350 poolC pelletA run1	1-350 poolC pelletA run2	350-589 poolB pelletA run1	350-589 poolB pelletA run2	350-589 poolC pelletA run1	350-589 poolC pelletA run2	Δ143-350 poolB pelletA run1	Δ143-350 poolB pelletA run2	Δ143-350 poolC pelletA run1	Δ143-350 poolC pelletA run2	Δ143-350 poolC pelletB run1	Δ143-350 poolC pelletB run2	1-350mNLS poolB pelletA run1	1-350mNLS poolB pelletA run2	1-350mNLS poolC pelletA run1	1-350mNLS poolC pelletA run2
Bait	59343	54607091	**SENP2**	265	216	294	279	184	169	212	226	146	91	191	175	940	781	357	304	853	890	658	523	798	730	119	125	82	81
Karyopherins	3837	19923142	KPNB1	230	205	263	247	227	224	287	285	360	262	531	510					181	206	320	234	562	494				
	3838	4504897	KPNA2	99	74	136	118	121	125	132	135	154	92	246	252					76	65	148	164	291	255				
	3839	34485722	KPNA3	45	32	83	77	44	44	52	58	79	54	114	117					33	23	74	71	108	121				
	3840	4504901	KPNA4	15	11	28	23	19	12	20	16	28	10	37	40					15	38	26	23	34	28				
	1434	29029559	CSE1L		6	9	9		6	6	6	24	11	34	38					15	12	11		9	12				
	10527	5453998	IPO7			10	5		4		6		8	24	15					24	12			13	10				
	30000	48675813	TNPO2 (KPNB2B)	10	12	10	6			16	13	29	15	53	53						2				9				
	3842	133925811	TNPO1 (KPNB2)	4	5		3					12	2	12	10									11					
	3836	222144293	KPNA1											4	4														
	23633	6912478	KPNA6											4	4														
Ran	5905	4506411	RANGAP1	13	11	14	19	14	16	22	22	59	34	32	32					8	10	9	3	11	6				
	729857	157266273	RGPD2			9	5	1	1		1	3	2	2	2							4		1	2				
FG Nucleoporins	5903	150418007	RANBP2/NUP358	49	47	30	38	33	27	39	48	158	100	135	125					24	31	31	20	45	25				34
	9972	24430146	NUP153	28	29	33	34	35	25	41	43	79	56	90	81							25	18	44	49				
	10762	24497451	NUP50			7	5			10	10	19	14	21	28							11	9	34	34				
Nup107-160 complex	55746	26051235	NUP133	4	3	5	3	4	3	5	5	13	19	18	17											4		5	
	57122	9966881	NUP107		3		4				12	19		10	16														
	23279	54859722	NUP160			6				7	6		7	11	5														
	4928	21264365	NUP96				6					7	8	11	12														
	79902	13376259	NUP85		1	4		5		5	5	7																	
SUMO	6613	54792069	SUMO-2/3[a]	3						6	3		10	7	4	134	112	236	132	11	7	23	23	15	20				
	7329	4507785	UBE2I	1						3	3																		
Other	6949	57164977	TCOF1	39	3					22	8	19		20	4	29	24			22	24	12	14	13		32		60	47
	51796	42542379	SRRM1				7		7	17			23			24	14			15	13					22		40	47
	23524	118572613	SRRM2	47		30							23			43	16			24						24	15	16	17
	1769	126012497	DNAH8		3					21		29		10	18									34		20	7	9	3
	129446	119372317	XIRP2	42	36	13	12	11		9	13	10	15				10	31	32	13	6	8	9	12	10	9			3
	6651	21040326	SON	13	18							3			18	87													
	5573	4506063	PRKAR1A		2										4														
	6780	82659083	STAU1		3																				3				
	23224	118918403	SYNE2						33																				

Flag-tagged SENP2 wild-type and indicated mutants were expressed in Flp-In T-REx 293 cells. Cells were lysed under nondenaturing conditions and Flag-tagged SENP2 and associated proteins were immunopurified using Flag-M2 agarose beads. Immunopurified proteins were eluted with ammonium hydroxide, digested with trypsin, and analyzed by LC-MS/MS. For protein identification, Thermo .RAW files were converted to the .mzXML format using Proteowizard, then searched using X!Tandem against the human (Human RefSeq Version 37) database. Spectral counts, corresponding to the number of times a peptide from each protein was observed, are indicated. Searched with GPM X!Tandem and analyzed with ProHits. GPM peptide cutoff value = −2.0.
aSUMO-2/3 identifications were combined. Both SUMO-2 and SUMO-3–specific peptides were observed.

TABLE 1: SENP2 interacts with soluble nuclear transport receptors and nucleoporins.
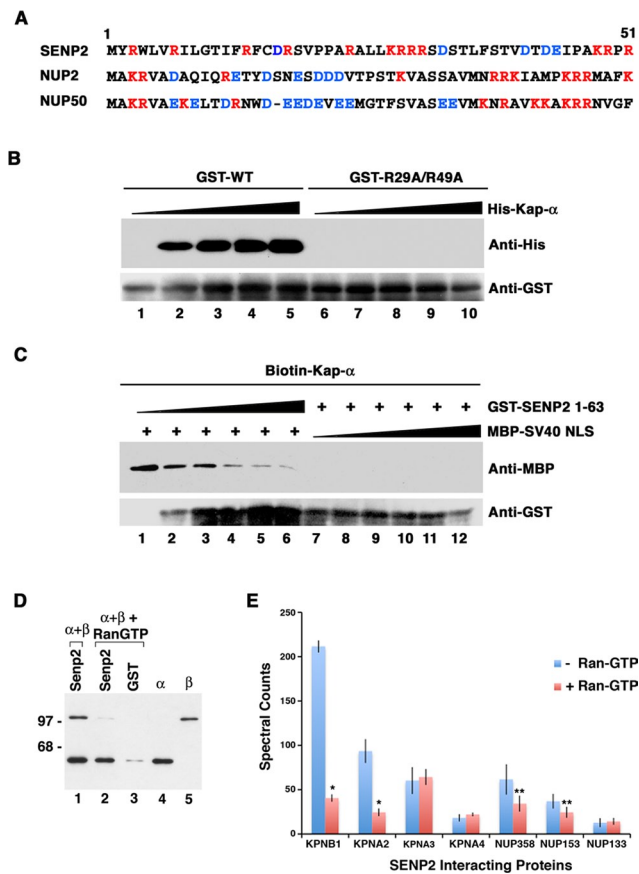
FIGURE 4: SENP2 interacts with karyopherin-α through a high-affinity NLS. (A) Alignment of the N-terminal nuclear localization sequences of SENP2, Nup2, and Nup50 with positively and negatively charged residues indicated in red and blue, respectively. (B) GST-tagged SENP2 1-63 wild-type (lanes 1–5) or NLS mutant SENP2 1-63(R29A/R49A) (lanes 6–10) were immobilized on glutathione beads and incubated with increasing concentrations of purified His-tagged karyopherin-α. Bound protein was eluted with SDS-sample buffer, resolved by SDS–PAGE, and analyzed by immunoblotting using GST- or His-specific antibodies. (C) MBP-tagged SV40 NLS was preincubated with biotinylated karyopherin-α. Increasing concentrations of GST-tagged SENP2 1-63 were subsequently incubated with the preformed karyopherin-α/NLS complexes and incubated for 1 h. Karyopherin-α and associated proteins were isolated using streptavidin beads and analyzed by immunoblotting with anti-MBP and -GST specific antibodies (lanes 1–6). The reciprocal experiment, in which GST-SENP2 1-63 was preincubated with biotinylated karyopherin-α and binding was subsequently challenged with increasing concentrations of MBP-SV40 NLS, was also performed (lanes 7–12). (D) GST-SENP2 or GST alone were immobilized on glutathione beads and incubated with His-tagged karyopherin-α and -β in the absence or presence of Ran-GTP, as indicated. Binding reactions were analyzed by immunoblotting with His-tag–specific antibodies. Karyopherin-α and -β were run alone as controls. Molecular-weight markers are indicated. (E) Immunoprecipitation MS analysis was performed using cell lysate prepared from cells expressing Flag-tagged, wild-type SENP2. Spectral counts obtained for each of the indicated interacting proteins obtained from immunopurifications performed in either the presence or absence of nonhydrolyzable Ran-GTP are plotted. Error bars represent the SE from four independent reactions (*p < 0.001; **p < 0.05).

were transiently expressed in HeLa cells. The SENP2 proteins were immunopurified and blots were probed with antibodies specific for karyopherin-α$_2$, karyopherin-β$_1$, FG-repeat nucleoporins recognized

by mAb 414, or Nup107. Consistent with the AP-MS results, full-length SENP2 copurified with karyopherin-α and -β, the FG repeat–containing nucleoporin Nup153, and also with Nup107 (Figure 5A, lane 7). Interactions with FG repeat–containing nucleoporins again appeared to be dependent on karyopherin binding, as mutating the NLS resulted in a loss of not only karyopherin-α and -β, but also Nup153 (Figure 5A, lane 8). Also consistent with the AP-MS analysis, interactions between SENP2 and Nup107 were unaffected by the NLS mutation (Figure 5A, lane 8).

Analysis of SENP2 1-63 and SENP2 1-63(R29A/R49A) revealed that the N-terminal 63 amino acids of SENP2 were sufficient for interactions with karyopherin-α and -β, and that these interactions were dependent upon the NLS (Figure 5A, lanes 9 and 10). Interactions with the FG-repeat nucleoporins Nup153 and Nup62 were also detected with the N-terminal 63 amino acids of SENP2. Interactions with Nup62 were not detected with full-length SENP2 (Figure 5A, lane 7), suggesting differences in NPC association compared with residues 1–63 alone. Nup107 did not copurify with the N-terminal 63 amino acids of SENP2, consistent with its interactions being mediated by a second targeting signal.

To further demonstrate the role of karyopherins in mediating interactions between SENP2 and FG-repeat nucleoporins, we performed in vitro binding assays using purified recombinant SENP2 1-63 and the FG-repeat domain of Nup153. GST-tagged SENP2 1-63 was immobilized on glutathione beads and incubated with the FG-repeat domain of Nup153 alone, together with karyopherin-α, or with both karyopherin-α and -β (Figure 5B). Interaction between SENP2 1-63 and the Nup153 FG-repeat domain was detected only in the presence of both karyopherin-α and -β, indicating that the NLS-dependent interaction between SENP2 and FG-repeat nucleoporins is mediated through association with nuclear transport receptors.

In addition to having an N-terminal NLS, SENP2 also contains a CRM1-dependent nuclear export signal (NES) between residues 317 and 332 (Itahana et al., 2006). To investigate whether both the NLS and the NES function cooperatively to affect SENP2 localization, we transfected cells with either wild-type SENP2, SENP2 NΔ66, or SENP2 NΔ66/NES (which contains leucine to alanine substitutions at NES residues 329 and 331; NΔ66 constructs were obtained from Itahana et al., 2006). Cells were then treated or not treated with the CRM1 inhibitor, leptomycin B (LMB). Whereas CRM1 inhibition caused no notable differences in the localization of wild-type SENP2, it caused a clear redistribution of SENP2 NΔ66 from the cytoplasm and NPCs to the nucleoplasm (Figure 5C). The effect of LMB on SENP2 NΔ66 was direct, as a similar change in localization was observed in cells expressing the SENP2 NΔ66/NES mutant. Thus the steady-state distribution of SENP2 among NPCs, the nucleus, and the cytoplasm is determined by both nuclear import and export receptors.

A second NPC-targeting signal mediates interactions between SENP2 and the Nup107-160 nucleoporin subcomplex

AP-MS analysis revealed that a SENP2 mutant lacking amino acids 143–350 interacted with karyopherins and FG repeat–containing nucleoporins, but not with members of the Nup107-160 subcomplex (Table 1). To further examine whether the residues within this region of SENP2 might mediate interactions with the Nup107-160 subcomplex, plasmids encoding GFP-tagged SENP2, SENP2 143-350, or SENP2 Δ144-349 were transiently expressed in HeLa cells, and interacting proteins were immunopurified. Immunopurified complexes were probed using antibodies specific for two members
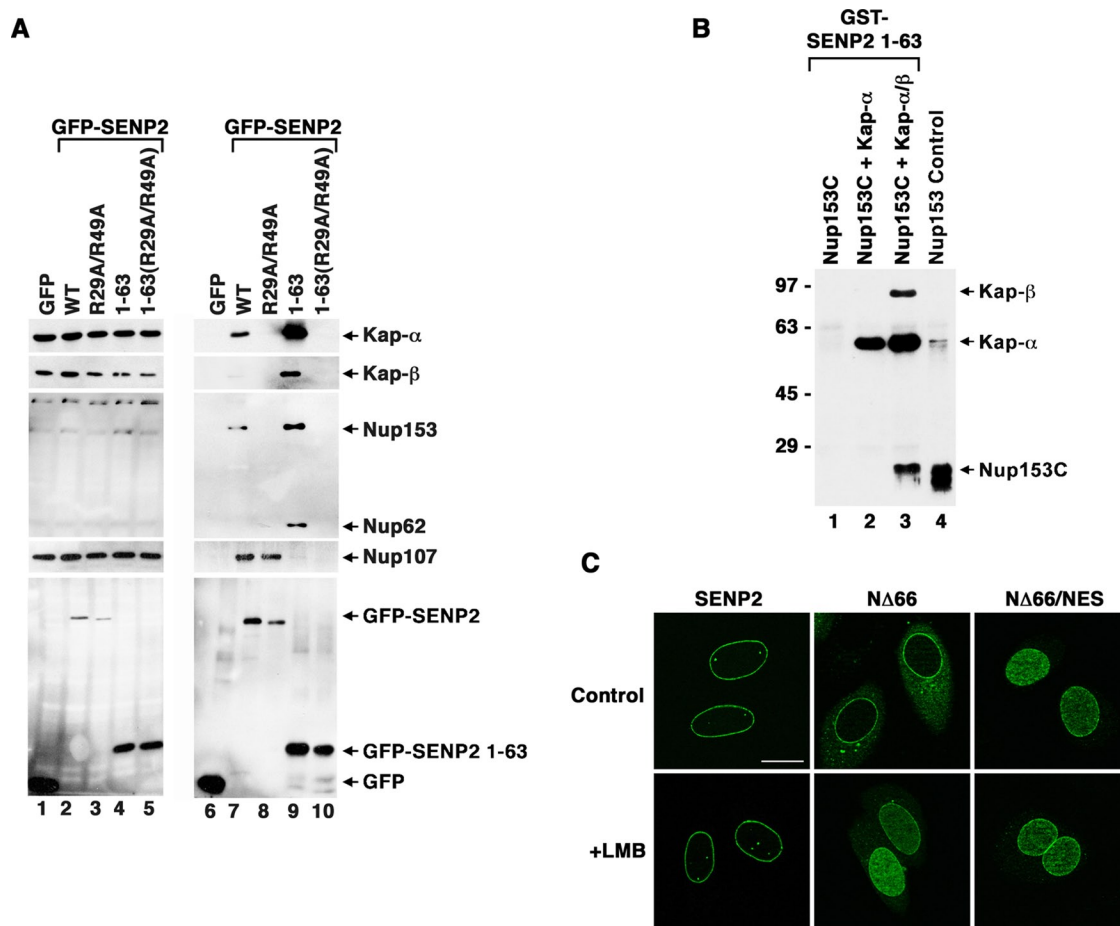
FIGURE 5: Nuclear transport receptors mediate interactions between SENP2 and the NPC. (A) HeLa cells were transfected with constructs encoding GFP, GFP-SENP2 (WT), GFP-SENP2(R29A/R49A), GFP-SENP2 1-63, or GFP-SENP2 1-63(R29A/R49A) for 36 h. Cells were lysed under nondenaturing conditions, and GFP-tagged proteins were immunopurified using a GFP-specific antibody. Cell lysates (lanes 1–5) and immunopurified proteins (lanes 6–10) were resolved by SDS–PAGE, and immunoblot analysis was performed with antibodies specific for karyopherin-α_2, karyopherin-β_1, Nup358/Nup153/Nup62 (mAb 414), Nup107, and GFP, as indicated. (B) Recombinant GST-tagged SENP2 1-63 was immobilized on glutathione beads and incubated with a His-tagged C-terminal FG-repeat domain of Nup153 (Nup153C) either alone, together with His-tagged karyopherin-α, or together with His-tagged karyopherin-α and -β. Bound proteins were eluted with SDS sample buffer, resolved by SDS–PAGE, and analyzed by immunoblotting using His-tag–specific antibodies. (C) HeLa cells transfected with GFP-SENP2, GFP-SENP2 NΔ66, or GFP-SENP2 NΔ66/NES (in which the NES between residues 317 and 332 was mutated), were treated with LMB or carrier (Control) for 40 min. Cells were analyzed by fluorescence microscopy.

of the Nup107-160 subcomplex, Nup107 and Nup96. Nup107 and Nup96 both copurified with full-length SENP2, and their association required residues 143–350 of SENP2, as deletion of these residues abrogated the interactions (Figure 6A, lanes 6 and 8). Moreover, the fragment of SENP2 containing residues 143–350 alone was sufficient for binding to the Nup107-160 subcomplex (Figure 6A, lane 7). Thus the association of SENP2 with the NPC is achieved through both karyopherin-mediated interactions with FG repeat–containing nucleoporins and association with the Nup107-160 subcomplex, as summarized in Figure 6B.

SENP2-targeting signals individually affect dynamic associations with NPCs

To investigate the dynamics of SENP2 interactions with NPCs, cells were transfected with a plasmid encoding full-length GFP-SENP2, and fluorescence recovery after photobleaching (FRAP) experiments were performed. A defined region of nuclear envelope was photobleached, images were collected at 2-s intervals following the initial

bleaching event, and the percentage of initial fluorescence was plotted versus time to a obtain FRAP recovery curve (Figure 7A). A rapid recovery to ~20% of the original signal was observed within the first minute, with little further recovery observed over an additional 2 min. This result suggests the existence of two pools of SENP2 at NPCs, one that is dynamic and one that is more stably bound. To investigate the contributions of the individual N-terminal targeting signals in determining SENP2 mobility, we performed FRAP analysis on cells expressing GFP-tagged SENP2 1-63 (containing just the NLS) or 1-350 (containing both the NLS and the Nup170-160 binding domain; Figure 7B). SENP2 1-63 recovered more quickly and more fully compared with SENP2 1-350, consistent with the targeting domains acting in a combinatorial manner to affect NPC association. SENP2 1-63 also recovered more quickly and fully relative to full-length SENP2, whereas the recovery of SENP2 1-350 was reduced.

To further investigate the contributions that the NLS and Nup107-160–binding domain make toward SENP2 association with NPCs,
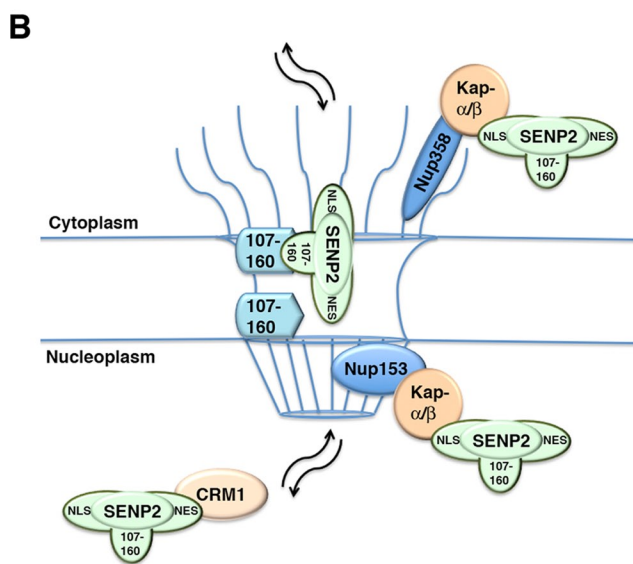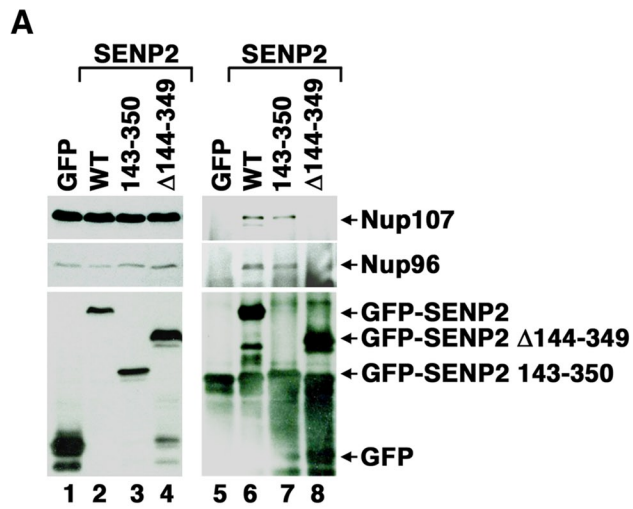
FIGURE 6: SENP2 contains a second NPC-targeting signal that mediates interactions with the Nup107-160 nucleoporin subcomplex. (A) HeLa cells were transfected with constructs encoding GFP, GFP-SENP2 (WT), GFP-SENP2 143-350, or GFP-SENP2 Δ144-349. Cells were lysed under nondenaturing conditions and proteins were immunopurified using GFP-specific antibodies. Cell lysates (lanes 1–4) and immunopurified proteins (lanes 5–8) were resolved by SDS–PAGE and analyzed by immunoblotting with Nup107-, Nup96- or GFP-specific antibodies. (B) Schematic representation summarizing the interactions affecting the association of SENP2 with NPCs.

we characterized the effects of ATP depletion on the localization of SENP2 1-63 and 1-350. ATP depletion results in a loss of Ran-GTP and a sequestration of karyopherin-α receptors in the nucleus (Schwoebel *et al.*, 2002). With this in mind, we anticipated that the karyopherin-α–dependent association of SENP2 1-63 with NPCs might be particularly sensitive to ATP depletion, whereas SENP2 1-350 might be less sensitive, due to associations with the Nup107-160 subcomplex. Cells were transiently transfected with constructs coding for GFP-tagged SENP2 1-63 and 1-350 and their localizations were determined in untreated cells and in cells treated with 2-deoxy-D-glucose and sodium azide to deplete ATP (Figure 7C). The localization of karyopherin-α3 was examined as an indicator of the efficiency of ATP depletion. In control cells, SENP2 1-63 was

detected at NPCs with a faint signal also visible in the nucleoplasm. Karyopherin-α3 was detected throughout the nucleoplasm and cytoplasm and also concentrated at NPCs. As anticipated, karyopherin-α3 shifted to the nucleoplasm in cells depleted of ATP. A shift in the distribution of SENP2 1-63 was also observed in ATP-depleted cells, with a notable increase in nucleoplasmic localization. The significance of this shift was verified by quantifying the ratio of NPC to nucleoplasmic signal in control and ATP-depleted cells (Figure 7D). Notably, NPC localization was not fully eliminated. In comparison with SENP2 1-63, SENP2 1-350 was concentrated approximately twofold higher at NPCs in untreated cells. A shift in distribution from NPCs was also detected upon ATP depletion; however, the ratio between NPCs and nucleoplasm remained nearly twice as high compared with SENP2 1-63 (Figure 7D). Together with the FRAP analysis, these results are consistent with the N-terminal NLS in SENP2 mediating a more dynamic association with NPCs, and with the Nup107-160 binding domain facilitating more stable associations.

SENP2 NPC-targeting signals function to restrict substrate accessibility

Mutations in yeast Ulp1 that affect its association with NPCs also affect its ability to access and desumoylate specific proteins (Li and Hochstrasser, 2003). To investigate the roles of NPC tethering on SENP2 substrate accessibility, we performed Western blot analysis on uninduced and induced stable cell lines expressing Flag-tagged, wild-type SENP2; SENP2 variants in which one or the other of the NPC-targeting signals was disrupted; and the catalytic domain alone (Figure 8B). Immunofluorescence microscopy (Figure 8A) and anti-Flag Western blotting (Figure 8B) verified the induced expression and localization of each protein. In comparison with uninduced cells, we observed no significant changes in overall sumoylation levels in cells induced to express wild-type SENP2. In contrast, we observed global decreases in high-molecular-weight SUMO-1 and SUMO-2/3 conjugates in cells induced to express SENP2 in which the Nup107-160 binding domain was deleted (Δ143-349) and in which the entire N-terminal domain was deleted (NΔ367). Thus NPC-targeting signals function to restrict substrate specificity through their effects on the steady-state association of SENP2 with NPCs.

DISCUSSION

SUMO-specific isopeptidases are found concentrated at NPCs in organisms ranging from yeast to human (Mukhopadhyay and Dasso, 2007). These isopeptidases are believed to define a functionally distinct subclass of desumoylating enzymes; however, their precise functions remain to be fully understood. In the current study, we have characterized the molecular interactions that mediate the association of SENP2 with NPCs in mammalian cells. We have demonstrated that the association of SENP2 with NPCs is mediated by a combination of interactions between soluble nuclear import and export receptors, peripherally associated nuclear basket proteins, and a core structural subcomplex of the NPC (Figure 6B). These interactions are mediated by three targeting signals in SENP2: a high-affinity NLS, a Nup107-160–binding element, and an NES. Our findings indicate that the precise location of SENP2 within cells and at NPCs is determined by the combined action of these targeting signals (Figure 6B).

SENP2 interactions with karyopherins

Among the most remarkable factors that we discovered affecting SENP2 association with NPCs is the association with soluble nuclear transport receptors. Our analysis revealed that SENP2 interacts with multiple members of the karyopherin family, including several
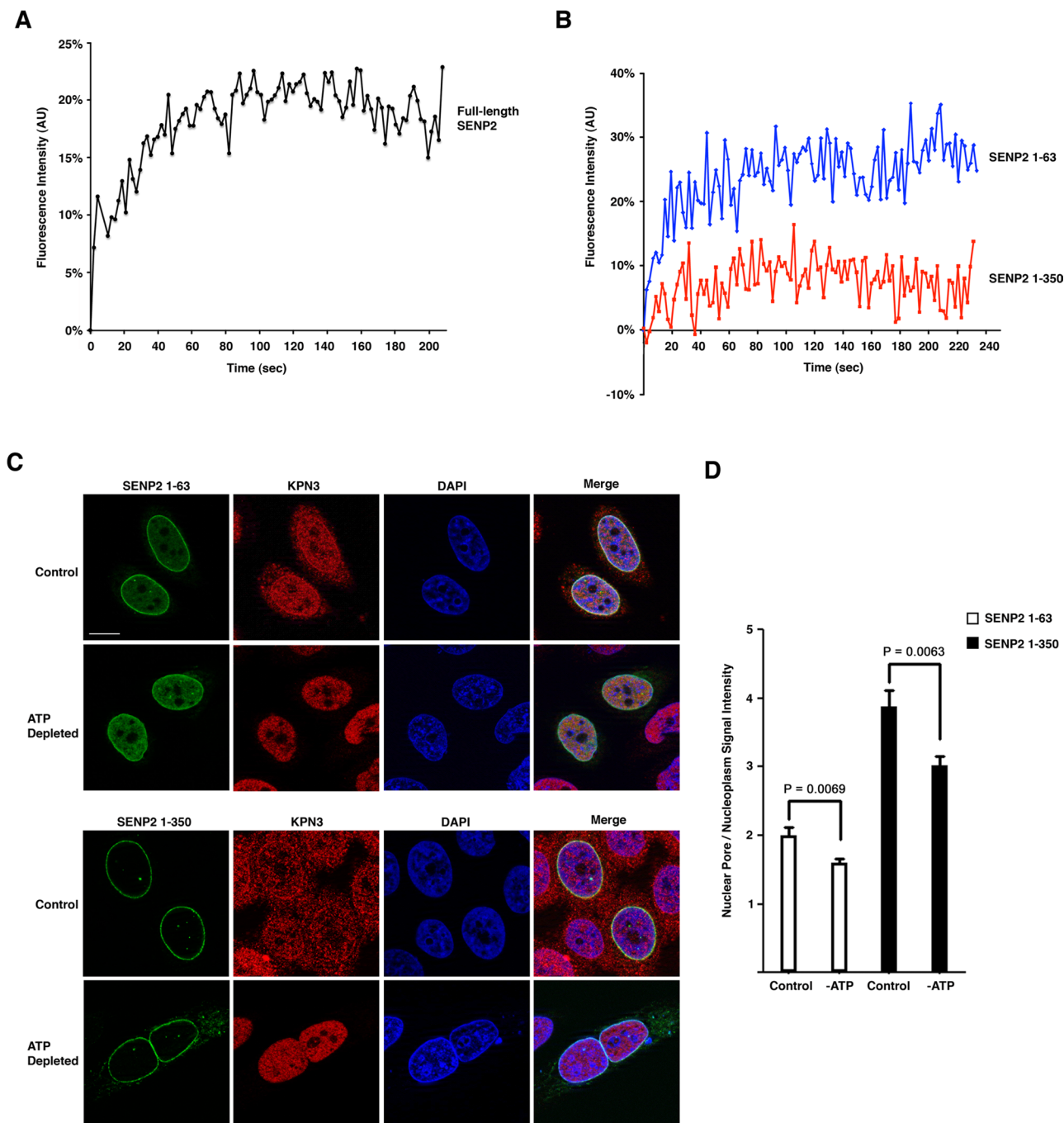
FIGURE 7: SENP2 is dynamically associated with NPCs. (A) A defined region of the nuclear envelope of GFP-SENP2–transfected cells was photobleached and images were collected every 2 s for 200 s. Fluorescence intensity after bleaching was normalized to 0%, and the relative recovery was plotted as a function of time. Average SE from 10 experiments was $\pm$ 3%. (B) FRAP analysis was performed as in (A), with cells transfected with GFP-SENP2 1-63 and 1-350. Average SEs from five experiments were $\pm$ 5% and $\pm$ 7% for cells expressing GFP-SENP2 1-63 and GFP-SENP2 1-350, respectively. (C) HeLa cells were transiently transfected with constructs encoding GFP-tagged SENP2 1-63 and 1-350. Cells were either untreated or treated with 2-deoxy-D-glucose and sodium azide to deplete ATP and stained with karyopherin-α_3–specific antibodies. Cells were analyzed by fluorescence microscopy. Scale bar: 10 µm. (D) The ratio of fluorescence intensities between NPCs and nucleoplasm was determined and plotted. Error bars represent the SE (n = 25).

karyopherin-αs (α_1, α_2, α_3, α_4, and α_6), as well as multiple karyopherin-βs (β_1, β_2, β_{2B}, importin-7, and CSE1L). Interactions with each of these transport receptors was dependent on the N-terminal NLS of SENP2, which we found to have an unusually high affinity for karyopherin-α. AP-MS analysis of SENP2 immunopurified from cell lysates in the presence of Ran-GTP revealed that only karyopherin-α_3

and -α_4 were resistant to dissociation. This suggests that, in vivo, karyopherin-α_3 and -α_4 selectively associate with SENP2 to affect its localization. Whether these two receptors, which form a distinct phylogenetic branch of the karyopherin-α family (Mason *et al.*, 2009), bind more tightly to SENP2 relative to other receptors remains to be determined. The dissociation of other karyopherins by
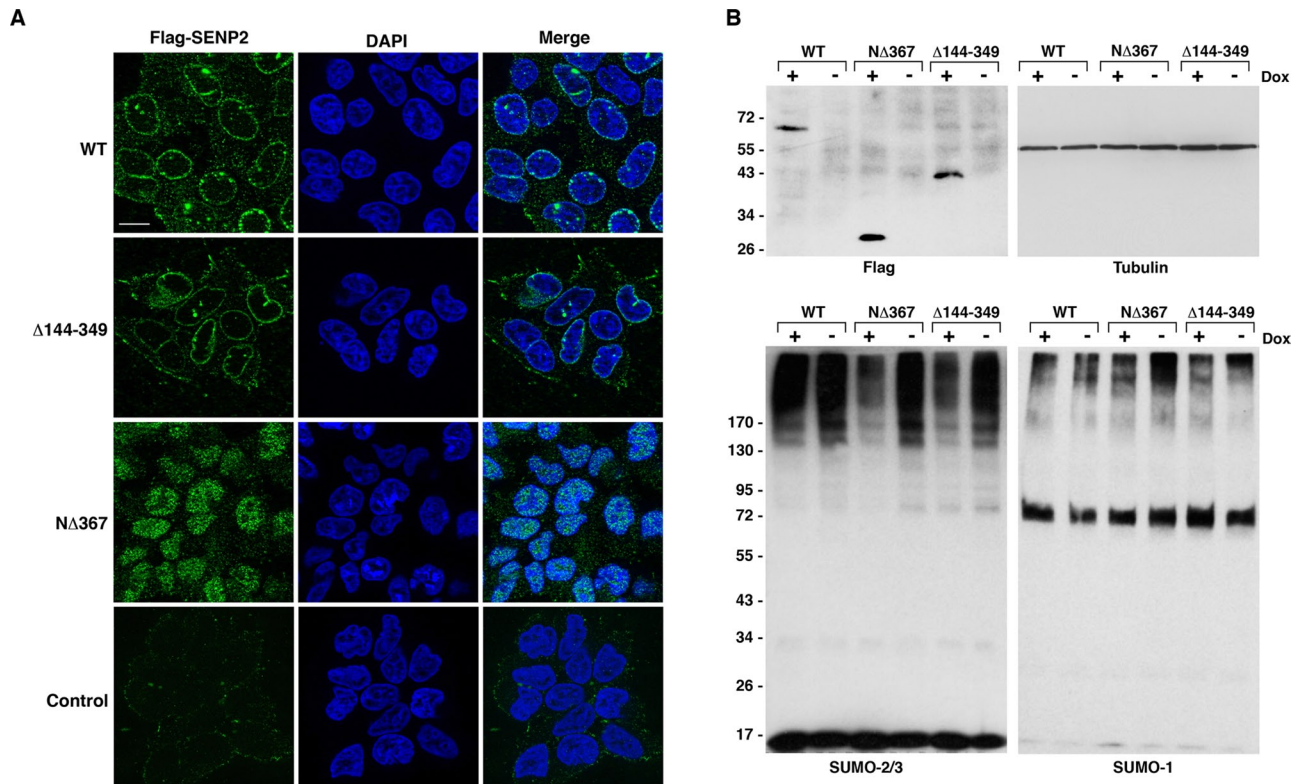
FIGURE 8: The NPC-targeting signals in SENP2 function to restrict substrate accessibility. Inducible stable cell lines for expressing Flag-tagged, wild-type SENP2, SENP2 Δ144-349, and SENP2 NΔ367 were cultured either in the absence or in the presence of doxycycline (Dox) to induce protein expression. (A) Induced cells were analyzed by immunofluorescence microscopy using anti-Flag–specific antibodies. Uninduced cells showed negligible background staining, as exemplified in the control. Scale bar: 10 μm. (B) Lysates were prepared from uninduced (−) and induced (+) cells, and equal quantities of total protein were analyzed by immunoblotting with antibodies specific for the Flag-tag, tubulin, SUMO-2/3, or SUMO-1. Molecular mass markers are indicated.

Ran-GTP suggests either an indirect association with SENP2, possibly through complexes of FG-repeat nucleoporins, or lower-affinity direct interactions. In addition to its N-terminal NLS, SENP2 also contains an NES that operates to limit accumulation in the nucleus and more generally to affect the distribution of SENP2 among NPCs, the nucleus, and the cytoplasm. Although this NES appears to be recognized by CRM1, based on LMB sensitivity (Figure 5C), we did not detect CRM1 in our AP-MS analysis, suggesting a transient or unstable interaction under the purification conditions used.

Like SENP2, the localization of yeast Ulp1 at NPCs is also dependent on unconventional interactions with multiple karyopherins, including karyopherin-α (Kap60) and karyopherin-β (Kap95), as well as karyopherin-121 (Kap121; Panse et al., 2003). In the case of Ulp1, these interactions are insensitive to dissociation by Ran-GTP. Similarly, we found that karyopherin-α interactions with SENP2 are unaffected by Ran-GTP, although karyopherin-β binding is affected. Insights into the exact molecular nature of the unusual interactions between karyopherins and Ulp1 and SENP2 will require further studies. Nonetheless, it appears that both Ulp1 and SENP2 form unusually stable associations with karyopherins that prevent their dissociation upon entry into the nucleus and thus enabling concentrations at NPCs. Consistent with this, SENP2 concentrates at the nucleoplasmic face of NPCs through interactions with Nup153 (Hang and Dasso, 2002; Zhang et al., 2002), and our findings demonstrate that this interaction is karyopherin-α/β dependent.

In addition to facilitating associations with NPCs, our findings also indicate that the N-terminal NLS of SENP2 is able to displace more traditional, lower-affinity NLS sequences from karyopherin-α. SENP2 could therefore function as a KaRF. KaRFs are proposed to function at the nucleoplasmic face of the NPC to facilitate dissociation of nuclear import cargoes from karyopherin-α and Ran-GTP initiated release of karyopherin-β (Gilchrist and Rexach, 2003; Matsuura and Stewart, 2005). KaRF proteins include yeast Nup2 and mammalian Nup50, proteins that, like SENP2, are dynamically associated with NPCs (Guan et al., 2000; Dilworth et al., 2001; Lindsay et al., 2002; Gilchrist and Rexach, 2003). This consideration raises the question of the precise functional significance of the interactions between nuclear transport receptors and Ulp1 and SENP2. Our studies provide clear evidence that karyopherin interactions affect the association of SENP2 with NPCs. However, it is possible that the interactions between SENP2 and karyopherins may also play a role in affecting karyopherin function. This is a particularly intriguing possibility, given the large number of different karyopherins associated directly or indirectly with SENP2. In addition to affecting substrate release through KaRF activity, SENP2 could also mediate the desumoylation of karyopherins and/or associated cargo proteins, thereby affecting their functions or transport. In the budding yeast, inhibition of sumoylation affects the nuclear import of proteins bearing classical NLSs and this inhibition is due in part to defects in the recycling of karyopherin-α (Kap60) from the nucleus to the cytoplasm (Stade et al., 2002). We have observed a similar effect on karyopherin-α recycling upon RNAi-mediated knockdown of Ubc9 in HeLa cells (unpublished data). The specific protein targets of sumoylation important for karyopherin-α recycling are not known;

however, it is intriguing to speculate that these targets are subject to regulation by SENP2- and Ulp1-mediated desumoylation.

SENP2 on and off the NPC

FRAP analysis revealed that a fraction of overexpressed GFP-SENP2 associates dynamically with NPCs. This mobility, and the previously reported finding that SENP2 shuttles between the nucleus and the cytoplasm (Itahana *et al.*, 2006), indicates that targets of SENP2 desumoylation may include proteins in both the cytoplasm and the nucleoplasm. In addition to the shuttling ability of full-length SENP2, we also detected multiple lower-molecular-weight isoforms of SENP2 potentially derived from alternatively spliced mRNAs. Based on their reactivity with SUMO-2-VS, each of the lower-molecular-weight forms of SENP2 have been determined to contain the C-terminal catalytic domain and are therefore likely to be missing elements from the N-terminal targeting domain. Consistent with this, alternative splicing in mouse cells generates multiple SENP2 isoforms with N-terminal deletions and notably distinct subcellular localizations to the cytoplasm and nucleus (Gong *et al.*, 2000; Nishida *et al.*, 2001; Best *et al.*, 2002). Two active human SENP2 variants are also predicted by the Celera Genomics genome sequencing project (GenBank accession numbers EAW78215 and EAW78216). These predicted isoforms include full-length SENP2 and a protein lacking the N-terminal 80 amino acids. The latter would be expected to share a localization pattern similar to our NΔ63 mutant, which was found at NPCs and in both the nucleus and cytoplasm (Figures 3B and 5C). Consistent with the expression of multiple SENP2 isoforms with distinct localizations, endogenous SENP2 was detected at NPCs, as well as in the nucleoplasm and cytoplasm (Figure 1C).

The association of Ulp1 with NPCs in yeast is subject to regulation. In mitosis, Ulp1 dissociates from NPCs and relocates in a Kap121-dependent manner to the septin ring, where it mediates desumoylation of the septin proteins (Makhnevych *et al.*, 2007). Similarly, Ulp1 dissociates from NPCs in response to ethanol stress and relocates to nucleoli in a manner dependent on Kap95 and Kap60 (Sydorskyy *et al.*, 2010). Our findings revealed that combinatorial effects of interactions with nuclear export and import factors and nucleoporins determine the precise localization of SENP2. Although inducible changes in SENP2 localization in interphase cells have not been reported, it is interesting to speculate that regulation of interactions between SENP2 and any one of the factors affecting NPC targeting could also affect substrate specificity. Consistent with this, our analysis of individual SENP2 mutants lacking the Nup107-160–binding domain or the entire N-terminus showed clear effects on cellular sumoylation levels and thus a connection between localization and substrate accessibility.

SENP2 interactions with the Nup107-160 nucleoporin subcomplex

In addition to their roles in NPC-related processes during interphase, nucleoporins have been implicated in mitotic processes related to chromosome segregation by a growing body of evidence (Wozniak *et al.*, 2010). Most notably, a fraction of the Nup107-160 nucleoporin subcomplex relocalizes to spindle fibers and to the outer-kinetochore plate during prophase, where it affects spindle assembly and establishment of microtubule/kinetochore attachments (Belgareh *et al.*, 2001; Loiodice *et al.*, 2004; Orjalo *et al.*, 2006; Wozniak *et al.*, 2010). Our finding that SENP2 interacts with the Nup107-160 subcomplex therefore has potentially important implications for understanding the molecular basis for the effects of this subcomplex on spindle and kinetochore function. Interestingly, we have previously found that overexpression of SENP2 leads to defects in microtubule/

kinetochore attachments, due to defects in the recruitment of CENP-E to the outer kinetochore (Zhang *et al.*, 2008). Thus, it is intriguing to speculate that some functions of the Nup107-160 subcomplex in mitosis may be affected through its association with SENP2.

The evolutionary conservation of SUMO-specific isopeptidases localized at NPCs implies important evolutionarily conserved functions for this subclass of isopeptidases. This implication is further underscored by our findings that the molecular mechanisms regulating the NPC associations of human SENP2 and yeast Ulp1 are also highly conserved. An important step toward understanding the critical functions of these isopeptidases lies in defining the specific subset of sumoylated proteins they regulate. Intriguingly, many of the nucleoporins and karyopherins that interact with SENP2 are also known to be sumoylated, suggesting that these proteins themselves may be substrates (Golebiowski *et al.*, 2009). Characterization of these potential SENP2 substrates, and other substrates both on and off the NPC, will be an important quest for future studies.

MATERIALS AND METHODS
Antibodies
SENP2-specific polyclonal antibodies were generated by immunizing rabbits with human SENP2 (residues 143–350) and affinity-purified using standard procedures. GFP-specific polyclonal antibodies were generated by immunizing rabbits with full-length recombinant GFP protein.

Nup107 polyclonal antibodies were a generous gift of Joseph Glavy (Stevens Institute of Technology, Hoboken, NJ). Nup96 polyclonal antibodies were provided by Beatriz Fontoura (University of Texas, Southwestern, Dallas, TX), and karyopherin-α_1 and -α_3 polyclonal antibodies were a generous gift from Stephen Adam (Northwestern University, Chicago, IL). Commercially available MBP (Zymed Laboratories, San Francisco, CA), karyopherin-β (Affinity Bio-Reagents, Golden, CO), and His-specific (GE Healthcare, Piscataway, NJ) antibodies were used. mAb 414 (recognizing the FG repeat–containing nucleoporins Nup358, Nup214, Nup153, and p62) was obtained from BAbCO (Richmond, CA).

Plasmid constructs
SENP2 cDNA was obtained as previously described (Zhang *et al.*, 2002). Full-length SENP2 or SENP2 truncation mutants were amplified using PCR and cloned into the pEGFP-C1 vector (Clontech, Mountain View, CA), using standard cloning procedures. Plasmids for SENP2-NΔ66 and NΔ66/ΔNES were kindly provided by Yanping Zhang (University of North Carolina, Chapel Hill, NC). The N-terminal 63 amino acids of SENP2 were subcloned into the pGEX 4T-1 vector (GE Healthcare) for bacterial expression. The NLS mutant of SENP2 (SENP2 1-63 R29A/R49A) was generated using PCR-based, site-directed mutagenesis. GFP-SENP1 vector was a gift from Mary Dasso (National Institutes of Health, Bethesda, MD). Mouse karyopherin-α_2 cDNA clone was amplified from a mouse fetal liver cDNA library (Invitrogen, Carlsbad, CA) and cloned into pET21a vector (EMD Biosciences, Gibbstown, NJ). Human karyopherin-β_1 was cloned into the pQE30 vector (Qiagen, Valencia, CA) for bacterial expression. Generation of the plasmid encoding His-tagged Nup153 (residues 1281–1475) was previously described (Zhang *et al.*, 2002).

Protein expression
A construct encoding GST-tagged SENP2 1-63 was transformed into *Escherichia coli* BL21 (CodonPlus; Stratagene, LaJolla, CA) cells, and expression was induced using 0.5 mM isopropylthiogalactoside. Cells were lysed in STE buffer (10 mM TrisHCl, pH 8.0, 1 mM EDTA, 150 mM NaCl, 1 mM phenylmethylsulfonyl fluoride [PMSF], 5 mg/ml

leupeptin and pepstatin A). Lysozyme (1 mg/ml) was added, and the mixture was incubated on ice for 15 min. A final concentration of 10 mM dithiothreitol (DTT) and 1.4% *N*-lauryl sarcosine (Sigma-Aldrich, St. Louis, MO) were added immediately prior to sonication. Lysate was sonicated four times at 15-s intervals and then centrifuged at $30,000 \times g$ for 20 min at 4°C. The supernatant was diluted 1:2 in fresh STE buffer and Triton-X 100 was added at a final concentration of 2%. The sample was incubated with glutathione–Sepharose beads (GE Healthcare), and bound protein was eluted in buffer containing 50 mM TrisHCl (pH 9.0) and 50 mM glutathione (Sigma-Aldrich). His-tagged mouse karyopherin-α_2, human karyopherin-β_1, and a C-terminal fragment of human Nup153 were purified using standard nickel–agarose affinity column chromatography, as recommended by the manufacturer (Qiagen). The plasmid encoding GST-tagged MBP-SV40 NLS was transformed into *E. coli* BL21 (Codon-Plus) cells; lysed in phosphate-buffered saline (PBS) containing 1 mM DTT, 0.5% Triton-X 100, 10% glycerol, 1 mg/ml lysozyme, 1:3000 dilution of Benzonase nuclease (Novagen, San Diego, CA), 1 mM PMSF, 1 μg/ml leupeptin and pepstatin A; and purified by affinity chromatography using glutathione–Sepharose beads (GE Healthcare). Protein was eluted by thrombin cleavage (GE Healthcare).

RanQ69L was purified essentially as described in Bischoff *et al.* (1994), with several modifications. Briefly, the clarified *E. coli* extract in lysis buffer (50 mM NaCl, 5 mM EDTA, 50 mM HEPES, 2 mM DTT, 1 mM 4-(2-aminoethyl) benzenesulfonyl fluoride, pH 7.6) was passed through a 10-ml diethylaminoethyl cellulose column equilibrated with buffer 1 (25 mM HEPES, 1 mM MgCl$_2$, 2 mM DTT, pH 7.6, 50 mM NaCl), and the flow-through was collected. This was then subjected to a 45% ammonium sulfate precipitation, which was followed by a 60% ammonium sulfate saturation of the 45% supernatant. The protein pellet from the 60% cut was dissolved in buffer 1 and separated on a Sephacryl S-100 column. The Ran-containing fractions were incubated on ice with 5 mM EDTA and 10 mM GTP for 1 h, then MgCl$_2$ was added at a final concentration of 20 mM. The GTP-loaded RanQ69L was then purified using a 25–800 mM linear NaCl gradient on a 25-ml SP-Sepharose FF column (GE Healthcare) equilibrated with buffer 1 containing 25 mM NaCl.

In vitro binding, NLS competition assays, and SUMO–vinyl sulfone reactions
To characterize interactions with karyopherins and Nup153, GST-tagged SENP2 1-63 or SENP2 1-63(R29A/R49A) was immobilized on glutathione–Sepharose beads (GE Healthcare) and nonspecific protein-binding sites were blocked by incubation in PBS containing 2% bovine serum albumin (BSA) for 20 min at 4°C. For karyopherin-α_2 binding, beads were incubated with increasing concentrations of purified His-tagged karyopherin-α_2 in binding buffer (0.1% Tween-20 in PBS) at room temperature for 1 h. Beads were washed six times with binding buffer, and bound proteins were eluted with SDS sample buffer. To assay for Nup153 binding, beads were incubated with a His-tagged, C-terminal fragment of Nup153 (amino acids 1287–1475) alone, in the presence of His-tagged karyopherin-α_2, or in the presence of His-karyopherin-α_2 and -β_1 in binding buffer (20 mM TrisHCl. pH 7.5, 150 mM NaCl, 0.1% Tween-20) for 30 min at room temperature. The beads were washed six times with binding buffer and the bound proteins were eluted with SDS sample buffer.

For NLS competition assays, His-tagged karyopherin-α_2 was biotinylated using EZ-Link Sulfo-NHS-LC-Biotin according to the manufacturer's protocol (Pierce, Rockford, IL). Recombinant MBP-SV40 NLS or GST-SENP2 1-63 was preincubated with the biotinylated karyopherin-α_2 in binding buffer (1% NP-40 in PBS) for 1 h at room

temperature. Increasing concentrations of the competing protein were then added directly to the preformed complexes and incubated for an additional 1 h at room temperature. Streptavidin–agarose beads (Pierce) were added to each reaction and incubated for 30 min at room temperature. Beads were washed six times with binding buffer, and bound proteins were eluted with SDS sample buffer.

To assay SENP2 reactivity with SUMO–vinyl sulfones, untransfected cells or cells transfected with the indicated plasmids were resuspended in reaction buffer (10 mM HEPES, pH 7.4, 150 mM NaCl, 5 mM EDTA, 1 mM DTT, 0.5% Triton-X 100, 1 μg/ml leupeptin and pepstatin A, 20 μg/ml aprotinin) and sonicated for 20 s. Lysates were centrifuged at $16,000 \times g$ for 10 min, and the protein concentration of the lysate was determined empirically. Protein concentration was maintained between 0.5 μg/ml and 2.0 μg/ml. HA-tagged SUMO-2-vinyl sulfone (Boston Biochem, Boston, MA) was diluted to 10 ng/μl in a buffer containing 10 mM HEPES (pH 7.4), 150 mM NaCl, 5 mM EDTA, 1 mM DTT, 10% glycerol. Diluted HA-SUMO-2-VS was added to the appropriate volume of cell lysate at a final concentration of 0.3 ng/μl and incubated for 30 min at room temperature. Reactions were terminated by addition of SDS sample buffer.

Stable cell lines
Tetracycline-inducible, Flag-tagged SENP2 proteins were expressed in human Flp-In T-REx 293 cells (Invitrogen). Protein expression was induced by adding 1 μg/ml tetracycline to the culture medium (DMEM + 10% fetal calf serum) for 24 h.

Cell culture, transfection, and RNA interference
HeLa or HEK293 cells were maintained at 37°C in DMEM supplemented with 10% fetal bovine serum, 10 mM HEPES (pH 8.0), and 1% penicillin–streptomycin. Cells were transfected using Lipofectamine 2000 according to the manufacturer's protocol (Invitrogen). siRNA oligos were used at a final concentration of 20 nM, unless otherwise indicated. SENP2 RNA oligo #1 (5'-GCCCAUG-GUAACUUCUGCUUGUAAU-3') was obtained from Invitrogen. SENP2 RNA oligo #2 (5'-AUAUCUGGAUUCUAUGGGAUU-3') was obtained from Ambion (Austin, TX). SENP2 RNA oligo #3 (5'-GC-CUAUUCAUCGGAAGGUAtt-3'), a Silencer Select Pre-designed siRNA, was obtained from Ambion.

For ATP-depletion experiments, HeLa cells were cultured in the presence of 6 mM 2-deoxy-D-glucose and 10 mM Na-azide for 1 h, as previously described (Schwoebel *et al.*, 2002). For LMB treatment, HeLa cells were transfected for 24 h with SENP2, SENP2 NΔ66, or SENP2 NΔ66/ΔNES, and then treated with 10 nM LMB (Sigma-Aldrich) for 40 min at 37°C. Cells were fixed and processed for fluorescence microscopy as described in *Immunofluorescence Microscopy*.

Immunoblotting and immunopurification
Immunoblot analysis was performed using enzyme-linked chemiluminescence ECL-Plus reagent (GE Healthcare). For immunopurification experiments involving GFP-tagged proteins, cells were lysed in buffer containing 50 mM TrisHCl (pH 7.5), 150 mM NaCl, 1 mM DTT, 5 mM EDTA, 1% Triton-X 100, 2 mM PMSF, and 10 mM NEM. Lysates were placed on ice for 5 min and then sonicated for 30 s and centrifuged at $16,000 \times g$ for 15 min. Lysate was incubated with GFP antibody–bound protein-A agarose beads (Santa Cruz Biotechnology, Santa Cruz, CA) for 6 h, and then beads were washed six times in PBS and bound proteins were eluted directly in SDS sample buffer.

For MS analysis of SENP2-interacting proteins, 6 × 150 cm² dishes of subconfluent (75–85%), stable, Flag-tagged SENP2-expressing cells were scraped into PBS, pooled, washed twice in 25 ml PBS, and collected by centrifugation at 1000 × *g* for 5 min at 4°C. Cell pellets were stored at −80°C. The cell pellet was weighed, and 1:4 pellet weight:volume lysis buffer was added. Lysis buffer consisted of 50 mM HEPES-NaOH (pH 8.0), 100 mM KCl, 2 mM EDTA, 0.1% NP40, 10% glycerol, 1 mM PMSF, 1 mM DTT, and 1:500 protease inhibitor cocktail (Sigma-Aldrich). On resuspension, cells were incubated on ice for 10 min, subjected to one additional freeze–thaw cycle, and then centrifuged at 27,000 × *g* for 20 min at 4°C. Supernatant was transferred to a fresh 15-ml conical tube, and 1:1000 benzonase nuclease (Novagen) plus 30 µl packed, preequilibrated Flag-M2 agarose beads (Sigma-Aldrich) were added. The mixture was incubated for 2 h at 4°C with end-over-end rotation. Beads were pelleted by centrifugation at 1000 × *g* for 1 min and transferred with 1 ml of lysis buffer to a fresh centrifuge tube. Beads were washed once with 1 ml lysis buffer and twice with 1 ml ammonium bicarbonate rinsing buffer (50 mM ammonium bicarbonate, pH 8.0, 75 mM KCl). Elution was performed by incubating the beads with 150 µl of 125 mM ammonium hydroxide (pH 11.0). The elution step was repeated twice. Eluate was centrifuged at 1000 × *g* for 1 min, transferred to a fresh centrifuge tube, and lyophilized. For Ran sensitivity assays, cleared lysates were spiked with 2 µM RanQ69L protein or an equal volume of vehicle (PBS pH 7.6), and affinity purification was conducted as above.

MS

One microgram MS-grade TPCK trypsin (Promega, Madison, WI) dissolved in 70 µl of 50 mM ammonium bicarbonate (pH 8.3) was added to the Flag eluate and incubated at 37°C overnight. The sample was lyophilized and brought up in buffer A (0.1% formic acid). LC analytical columns (75-mm inner diameter) and precolumns (100-mm inner diameter) were made in-house from fused silica capillary tubing from InnovaQuartz (Phoenix, AZ) and packed with 100 Å C$_{18}$–coated silica particles (Magic, Michrom Bioresources, Auburn, CA). Peptides were subjected to LC-electrospray ionization–MS/MS, using a 120-min reverse-phase LC (95% water–95% acetonitrile, 0.1% formic acid) buffer gradient running at 250 nl/min on a Proxeon EASY-nLC pump in-line with a hybrid LTQ-Orbitrap mass spectrometer (Thermo Fisher Scientific, Waltham, MA). A parent ion scan was performed in the Orbitrap using a resolving power of 30,000, then the six most intense peaks were selected for MS/MS (minimum ion count of 1000 for activation), using standard collision-induced dissociation fragmentation. Fragment ions were detected in the LTQ. Dynamic exclusion was activated such that MS/MS of the same *m/z* (within a range of −0.1 to +2.1 Thomson units; exclusion list size = 500) detected three times within 45 s were excluded from analysis for 60 s. For protein identification, Thermo .RAW files were converted to the .mzXML format using Proteowizard (Kessner *et al.*, 2008), then searched using X!Tandem (Craig and Beavis, 2004) against the human (Human RefSeq Version 37) database. X!Tandem search parameters were: complete modifications, none; cysteine modifications, none; potential modifications, +16@M and W, +32@M and W, +42@N-terminus, +1@N and Q. Each immunopurification sample was analyzed using multiple technical replicates. Data were analyzed using the ProHits software tool (Liu *et al.*, 2010). Proteins identified with an X!Tandem expect score of −2.0 or lower and detected only in the SENP2 AP-MS analyses are reported.

Immunofluorescence microscopy

HeLa cells were cultured on glass coverslips, fixed in 2% formaldehyde for 30 min at room temperature, and permeabilized in 0.5% Triton-X 100. Immunostaining was carried out as previously described (Matunis *et al.*, 1996). Images were collected using a Zeiss ObserverZ1 fluorescence microscope with an Apotome VH optical sectioning grid. Images were processed using AxioVision Software Release 4.8.1 (Zeiss, Jena, Germany).

For quantitative analysis of fluorescence intensities, acquired images were analyzed using ImageJ (Abramhoff *et al.*, 2004). Two rectangular regions of equal dimensions were drawn at either the nuclear envelope or within the nucleoplasm of a cell. The pixel intensities were measured, and ratios were determined for 25 individual cells. Average ratios and SEs were graphed.

FRAP

Cells were cultured in 35-mm glass-bottom dishes (MatTek, Ashland, MA). At 24 h following transfection, FRAP experiments were performed on a Zeiss LSM510 confocal microscope using a Plan-Apochromat 63×/1.4 oil objective and a pinhole open to 134 µm. A defined region of the nuclear envelope was photobleached using a 488-nm laser at 1.5% power, and then images were acquired every 2 s postbleaching. Fluorescence intensity within the defined region, as well as an equivalent-sized region in an adjacent cell, was quantified using the LSM Image browser software. No significant background photobleaching was detected in the neighboring cells. The signal intensity after photobleaching within the defined region was normalized to 0%, and the relative recovery of fluorescence intensity was plotted versus time. Data were obtained for 5–10 cells for each sample, and the normalized fluorescence intensities were averaged and plotted. An average SE of ± 3% was obtained for the full-length SENP2, while average standard errors of ± 5% and ± 7% were obtained for SENP2 1-63 and 1-350, respectively.

REFERENCES

Abramhoff MD, Magelhaes PJ, Ran SJ (2004). Image processing with ImageJ. Biophotonics Int 11, 36–42.

Bailey D, O'Hare P (2004). Characterization of the localization and proteolytic activity of the SUMO-specific protease, SENP1. J Biol Chem 279, 692–703.

Belgareh N *et al.* (2001). An evolutionarily conserved NPC subcomplex, which redistributes in part to kinetochores in mammalian cells. J Cell Biol 154, 1147–1160.

Best JL, Ganiatsas S, Agarwal S, Changou A, Salomoni P, Shirihai O, Meluh PB, Pandolfi PP, Zon LI (2002). SUMO-1 protease-1 regulates gene transcription through PML. Mol Cell 10, 843–855.

Bischoff FR, Klebe C, Kretschmer J, Wittinghofer A, Ponstingl H (1994). RanGAP1 induces GTPase activity of nuclear Ras-related Ran. Proc Natl Acad Sci USA 91, 2587–2591.

Brohawn SG, Partridge JR, Whittle JR, Schwartz TU (2009). The nuclear pore complex has entered the atomic age. Structure 17, 1156–1168.

Craig R, Beavis RC (2004). TANDEM: matching proteins with tandem mass spectra. Bioinformatics 20, 1466–1467.

Davis LI, Blobel G (1986). Identification and characterization of a nuclear pore complex protein. Cell 45, 699–709.

Dilworth DJ, Suprapto A, Padovan JC, Chait BT, Wozniak RW, Rout MP, Aitchison JD (2001). Nup2p dynamically associates with the distal regions of the yeast nuclear pore complex. J Cell Biol 153, 1465–1478.

Geiss-Friedlander R, Melchior F (2007). Concepts in sumoylation: a decade on. Nat Rev Mol Cell Biol 8, 947–956.

Gilchrist D, Mykytka B, Rexach M (2002). Accelerating the rate of disassembly of karyopherin.cargo complexes. J Biol Chem 277, 18161–18172.

Gilchrist D, Rexach M (2003). Molecular basis for the rapid dissociation of nuclear localization signals from karyopherin α in the nucleoplasm. J Biol Chem 278, 51937–51949.

Gingras AC, Gstaiger M, Raught B, Aebersold R (2007). Analysis of protein complexes using mass spectrometry. Nat Rev Mol Cell Biol 8, 645–654.

Golebiowski F, Matic I, Tatham MH, Cole C, Yin Y, Nakamura A, Cox J, Barton GJ, Mann M, Hay RT (2009). System-wide changes to SUMO modifications in response to heat shock. Sci Signal 2, ra24.

Gong L, Millas S, Maul GG, Yeh ET (2000). Differential regulation of sentrinized proteins by a novel sentrin-specific protease. J Biol Chem 275, 3355–3359.

Gong L, Yeh ET (2006). Characterization of a family of nucleolar SUMO-specific proteases with preference for SUMO-2 or SUMO-3. J Biol Chem 281, 15869–15877.

Guan T, Kehlenbach RH, Schirmer EC, Kehlenbach A, Fan F, Clurman BE, Arnheim N, Gerace L (2000). Nup50, a nucleoplasmically oriented nucleoporin with a role in nuclear protein export. Mol Cell Biol 20, 5619–5630.

Hang J, Dasso M (2002). Association of the human SUMO-1 protease SENP2 with the nuclear pore. J Biol Chem 277, 19961–19966.

Itahana Y, Yeh ET, Zhang Y (2006). Nucleocytoplasmic shuttling modulates activity and ubiquitination-dependent turnover of SUMO-specific protease 2. Mol Cell Biol 26, 4675–4689.

Johnson ES (2004). Protein modification by SUMO. Annu Rev Biochem 73, 355–382.

Kang X, Qi Y, Zuo Y, Wang Q, Zou Y, Schwartz RJ, Cheng J, Yeh ET (2010). SUMO-specific protease 2 is essential for suppression of polycomb group protein-mediated gene silencing during embryonic development. Mol Cell 38, 191–201.

Kessner D, Chambers M, Burke R, Agus D, Mallick P (2008). ProteoWizard: open source software for rapid proteomics tools development. Bioinformatics 24, 2534–2536.

Kroetz MB, Su D, Hochstrasser M (2009). Essential role of nuclear localization for yeast Ulp2 SUMO protease function. Mol Biol Cell 20, 2196–2206.

Lewis A, Felberbaum R, Hochstrasser M (2007). A nuclear envelope protein linking nuclear pore basket assembly, SUMO protease regulation, and mRNA surveillance. J Cell Biol 178, 813–827.

Li SJ, Hochstrasser M (1999). A new protease required for cell-cycle progression in yeast. Nature 398, 246–251.

Li SJ, Hochstrasser M (2000). The yeast ULP2 (SMT4) gene encodes a novel protease specific for the ubiquitin-like Smt3 protein. Mol Cell Biol 20, 2367–2377.

Li SJ, Hochstrasser M (2003). The Ulp1 SUMO isopeptidase: distinct domains required for viability, nuclear envelope localization, and substrate specificity. J Cell Biol 160, 1069–1081.

Lindsay ME, Plafker K, Smith AE, Clurman BE, Macara IG (2002). Npap60/Nup50 is a tri-stable switch that stimulates importin-α:β-mediated nuclear protein import. Cell 110, 349–360.

Liu G et al. (2010). ProHits: integrated software for mass spectrometry-based interaction proteomics. Nat Biotechnol 28, 1015–1017.

Loiodice I, Alves A, Rabut G, Van Overbeek M, Ellenberg J, Sibarita JB, Doye V (2004). The entire Nup107–160 complex, including three new members, is targeted as one entity to kinetochores in mitosis. Mol Biol Cell 15, 3333–3344.

Makhnevych T, Ptak C, Lusk CP, Aitchison JD, Wozniak RW (2007). The role of karyopherins in the regulated sumoylation of septins. J Cell Biol 177, 39–49.

Makhnevych T et al. (2009). Global map of SUMO function revealed by protein-protein interaction and genetic networks. Mol Cell 33, 124–135.

Mason DA, Stage DE, Goldfarb DS (2009). Evolution of the metazoan-specific importin α gene family. J Mol Evol 68, 351–365.

Matsuura Y, Lange A, Harreman MT, Corbett AH, Stewart M (2003). Structural basis for Nup2p function in cargo release and karyopherin recycling in nuclear import. EMBO J 22, 5358–5369.

Matsuura Y, Stewart M (2005). Nup50/Npap60 function in nuclear protein import complex disassembly and importin recycling. EMBO J 24, 3681–3689.

Matunis MJ, Coutavas E, Blobel G (1996). A novel ubiquitin-like modification modulates the partitioning of the Ran-GTPase-activating protein RanGAP1 between the cytosol and the nuclear pore complex. J Cell Biol 135, 1457–1470.

Mukhopadhyay D, Ayaydin F, Kolli N, Tan SH, Anan T, Kametaka A, Azuma Y, Wilkinson KD, Dasso M (2006). SUSP1 antagonizes formation of highly SUMO2/3-conjugated species. J Cell Biol 174, 939–949.

Mukhopadhyay D, Dasso M (2007). Modification in reverse: the SUMO proteases. Trends Biochem Sci 32, 286–295.

Nagai S, Dubrana K, Tsai-Pflugfelder M, Davidson MB, Roberts TM, Brown GW, Varela E, Hediger F, Gasser SM, Krogan NJ (2008). Functional targeting of DNA damage to a nuclear pore-associated SUMO-dependent ubiquitin ligase. Science 322, 597–602.

Nishida T, Kaneko F, Kitagawa M, Yasuda H (2001). Characterization of a novel mammalian SUMO-1/Smt3-specific isopeptidase, a homologue of rat axam, which is an axin-binding protein promoting β-catenin degradation. J Biol Chem 276, 39060–39066.

Nishida T, Tanaka H, Yasuda H (2000). A novel mammalian Smt3-specific isopeptidase 1 (SMT3IP1) localized in the nucleolus at interphase. Eur J Biochem 267, 6423–6427.

Orjalo AV, Arnaoutov A, Shen Z, Boyarchuk Y, Zeitlin SG, Fontoura B, Briggs S, Dasso M, Forbes DJ (2006). The Nup107–160 nucleoporin complex is required for correct bipolar spindle assembly. Mol Biol Cell 17, 3806–3818.

Palancade B, Liu X, Garcia-Rubio M, Aguilera A, Zhao X, Doye V (2007). Nucleoporins prevent DNA damage accumulation by modulating Ulp1-dependent sumoylation processes. Mol Biol Cell 18, 2912–2923.

Panse VG, Kuster B, Gerstberger T, Hurt E (2003). Unconventional tethering of Ulp1 to the transport channel of the nuclear pore complex by karyopherins. Nat Cell Biol 5, 21–27.

Pichler A, Gast A, Seeler JS, Dejean A, Melchior F (2002). The nucleoporin RanBP2 has SUMO1 E3 ligase activity. Cell 108, 109–120.

Schwoebel ED, Ho TH, Moore MS (2002). The mechanism of inhibition of Ran-dependent nuclear transport by cellular ATP depletion. J Cell Biol 157, 963–974.

Smith M, Bhaskar V, Fernandez J, Courey AJ (2004). Drosophila Ulp1, a nuclear pore-associated SUMO protease, prevents accumulation of cytoplasmic SUMO conjugates. J Biol Chem 279, 43805–43814.

Stade K, Vogel F, Schwienhorst I, Meusser B, Volkwein C, Nentwig B, Dohmen RJ, Sommer T (2002). A lack of SUMO conjugation affects cNLS-dependent nuclear protein import in yeast. J Biol Chem 277, 49554–49561.

Strambio-De-Castillia C, Niepel M, Rout MP (2010). The nuclear pore complex: bridging nuclear transport and gene regulation. Nat Rev Mol Cell Biol 11, 490–501.

Sydorskyy Y, Srikumar T, Jeram SM, Wheaton S, Vizeacoumar FJ, Makhnevych T, Chong YT, Gingras AC, Raught B (2010). A novel mechanism for SUMO system control: regulated Ulp1 nucleolar sequestration. Mol Cell Biol 30, 4452–4462.

Terry LJ, Shows EB, Wente SR (2007). Crossing the nuclear envelope: hierarchical regulation of nucleocytoplasmic transport. Science 318, 1412–1416.

Wozniak R, Burke B, Doye V (2010). Nuclear transport and the mitotic apparatus: an evolving relationship. Cell Mol Life Sci 67, 2215–2230.

Xu XM, Rose A, Muthuswamy S, Jeong SY, Venkatakrishnan S, Zhao Q, Meier I (2007). NUCLEAR PORE ANCHOR, the Arabidopsis homolog of Tpr/Mlp1/Mlp2/megator, is involved in mRNA export and SUMO homeostasis and affects diverse aspects of plant development. Plant Cell 19, 1537–1548.

Zhang H, Saitoh H, Matunis MJ (2002). Enzymes of the SUMO modification pathway localize to filaments of the nuclear pore complex. Mol Cell Biol 22, 6498–6508.

Zhang XD, Goeres J, Zhang H, Yen TJ, Porter AC, Matunis MJ (2008). SUMO-2/3 modification and binding regulate the association of CENP-E with kinetochores and progression through mitosis. Mol Cell 29, 729–741.

Zhao X, Blobel G (2005). A SUMO ligase is part of a nuclear multiprotein complex that affects DNA repair and chromosomal organization. Proc Natl Acad Sci USA 102, 4777–4782.

Zhao X, Wu CY, Blobel G (2004). Mlp-dependent anchorage and stabilization of a desumoylating enzyme is required to prevent clonal lethality. J Cell Biol 167, 605–611.